The Causes of Horizontal-Vertical (H-V) Bias in Optical Lithography

Chris A. Mack
KLA-Tencor, FINLE Division

Abstract

Horizontal-Vertical (H-V) bias is the systematic difference in linewidth between closely located horizontally and vertically oriented resist features that, other than orientation, should be identical. There are two major causes of H-V bias: astigmatism, which causes an H-V bias that varies through focus, and illumination source aberrations such as a illumination telecentricity error. In this paper, each of these mechanisms are explored and analyzed. For astigmatism, an analytic expression for amount of H-V bias is developed. For illumination telecentricity error, simulations are used to show the partial coherence, feature size, and pitch dependencies. An expression for the pitch which gives the worst H-V bias in the presence of illumination telecentricity error is presented.

Keywords: H-V bias, CD control, lithography modeling, PROLITH

1. Introduction

One nanometer of critical dimension (CD) error is no longer in the noise for sub-100nm processes. While just a few years ago an error source that contributed one nanometer to the CD error budget would be swamped by other 10nm error sources of the process, today the total CD error budget for a 65nm gate process can be ±4nm. At this level, a one nanometer CD error is significant, especially if it is systematic.

One of the systematic sources of CD errors receiving renewed scrutiny in recent years is called horizontal-vertical (H-V) bias. Quite simply, H-V bias is the systematic difference in linewidth between closely located horizontally and vertically oriented resist features that, other than orientation, should be identical. H-V bias has always been a concern in optical lithography, but it has tended to be one of the "second order" errors that rarely limits overall lithographic capability. It's not clear, however, whether H-V bias will retain its second tier status in the 65nm and 45nm generations, or graduate to a first tier concern.

There are two main causes of H-V bias. The first and most well known cause is astigmatism and related aberrations. The second is illumination source shape aberrations such as an illumination telecentricity error (causing the source to be not centered in the pupil). These two sources of H-V bias will be explored in detail in the sections below.

2. Astigmatism

The aberration of astigmatism results in a difference in best focus as a function of the orientation of the feature. Using the Zernike polynomial description of aberrations, 3rd order 90° astigmatism (which affects horizontally and vertically oriented lines) takes the form

$$phase\ error = 2\pi Z_{astig} R^2 \cos 2\theta \qquad (1)$$

where (R,θ) are polar coordinates in the pupil plane (R being defined relative to the numerical aperture and ranging from zero to one) and Z_{astig} is the Zernike coefficient in units of fractions of a wavelength. A picture of this phase error across the pupil is shown in Figure 1.

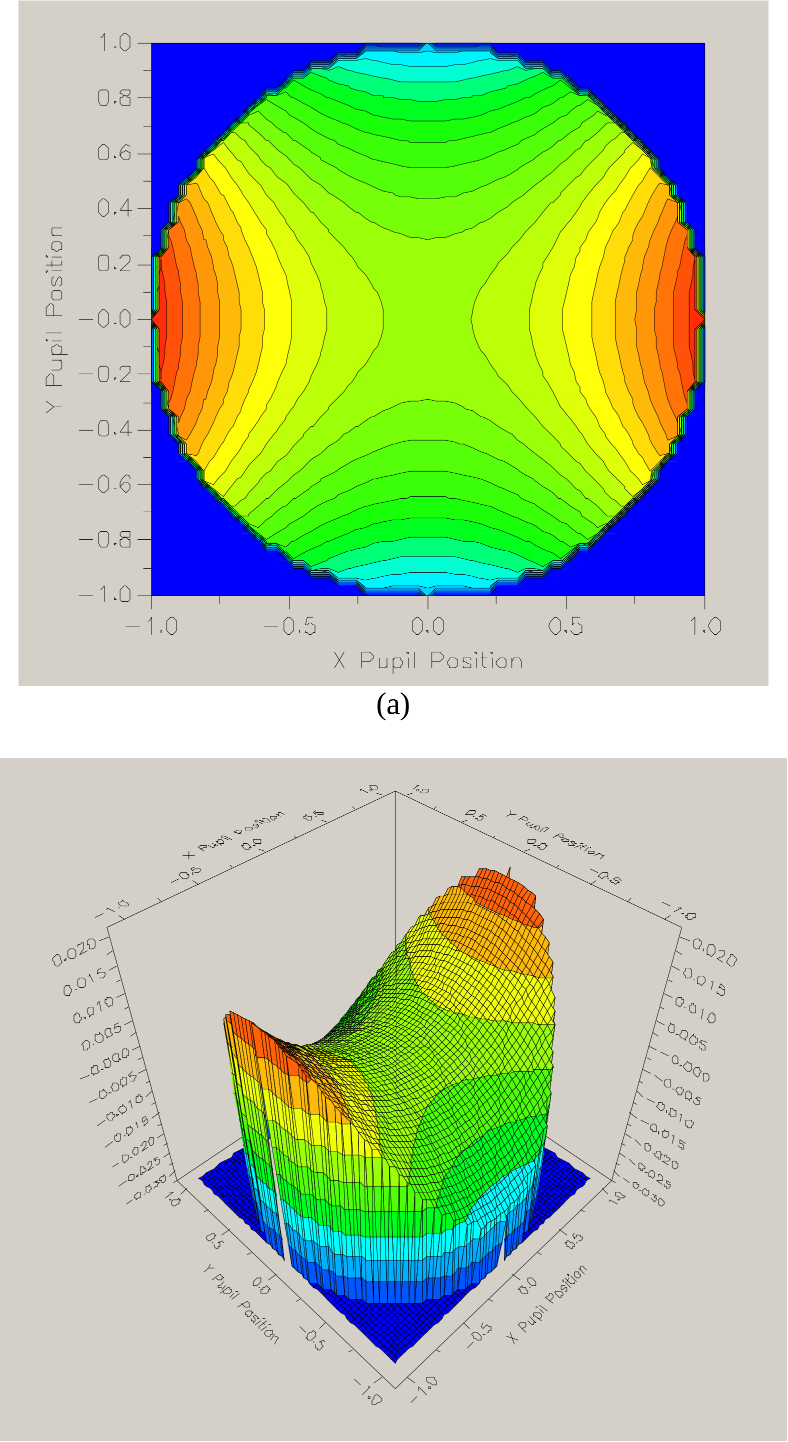

(a)

(b)

Figure 1. Plot of the phase error across the objective lens pupil for 0.02 waves of 90º astigmatism: a) contour plot, and b) 3D plot.

Consider a vertically, *y*-oriented pattern of lines and spaces. The diffraction pattern will spread across the *x*-axis of the pupil, corresponding to $\theta = 0^o$ and 180^o. Thus, the phase error will be $2\pi Z_{astig}R^2$ for this feature. The R^2 dependence of the phase error immediately brings to mind defocus. A common way to think about defocus is to describe it as an aberration. By viewing the actual wavefront exiting the lens (and focusing some defocus distance away from the wafer) as having an error in curvature relative to the desired wavefront (i.e., the one that focuses on the wafer), we can quantify the effect of defocus. From this analysis, the phase error due to defocus is

$$phase\ error \approx \frac{\pi \delta NA^2}{\lambda} R^2 \tag{2}$$

where δ is the defocus distance, λ is the wavelength, and *NA* is the numerical aperture. (Equation (2) is approximate because it retains only the first term in a Taylor series. While this approximation is progressively less accurate for higher numerical apertures, it will be good enough for our purposes.) Immediately, one sees that 3rd order astigmatism looks just like the approximate effect of defocus. Thus, equating the phase error from equations (2) and (3), astigmatism will cause the vertically oriented lines to shift best focus by an amount

$$\Delta\delta_{vert} \approx \frac{2Z_{astig}\lambda}{NA^2} \tag{3}$$

For horizontally oriented lines, the diffraction pattern will be along the *y*-axis of the pupil ($\theta = \pm 90^o$) and the astigmatism will cause a phase error of $-2\pi Z_{astig}R^2$. Thus, the focus shift for the horizontal lines will be the same magnitude as given by equation (3), but in the opposite direction.

To see how astigmatism causes H-V bias, we need to understand how a shift in focus might affect the resist feature CD. To first order, CD has a quadratic dependence on focus.

$$CD \approx CD_{best\ focus} + a\delta^2 \tag{4}$$

where *a* is the dose-dependent curvature of the CD through focus curve. Recalling the typical shapes of Bossung curves, *a* can vary from positive to negative values as a function of dose. If best focus is shifted due to astigmatism, we can calculate the CD of the vertical and horizontal features by adding the focus shift of equation (3) to equation (4).

$$\begin{aligned} CD_{vert} &\approx CD_{best\ focus} + a\left(\delta - \frac{2Z_{astig}\lambda}{NA^2}\right)^2 \\ CD_{horiz} &\approx CD_{best\ focus} + a\left(\delta + \frac{2Z_{astig}\lambda}{NA^2}\right)^2 \end{aligned} \tag{5}$$

From, here a straightforward subtraction gives us the H-V bias:

$$H - V\ bias \approx \frac{8a\delta Z_{astig}\lambda}{NA^2} \qquad (5)$$

The H-V bias is directly proportional to the amount of astigmatism in the lens (Z_{astig}) and to the curvature of the CD-through-focus curve (a). But it is also directly proportional to the amount of defocus. In fact, a plot of H-V bias through focus is a sure way to identify astigmatism (so long as you don't use the isofocal dose, where $a \approx 0$, for the experiment). Figure 2 shows some typical results (using simulation to mimic the experiment). Note that the isolated lines show a steeper slope than the dense lines due to a larger value of the CD through focus curvature. In fact, if a is determined by fitting equation (4) to measured CD through focus data, a reasonable estimate of Z_{astig} can be made using an experimentally measured H-V bias through focus curve. Note also that the true shape of the curves in Figure 2 is only approximately linear, since both equations (3) and (4) ignore higher order terms.

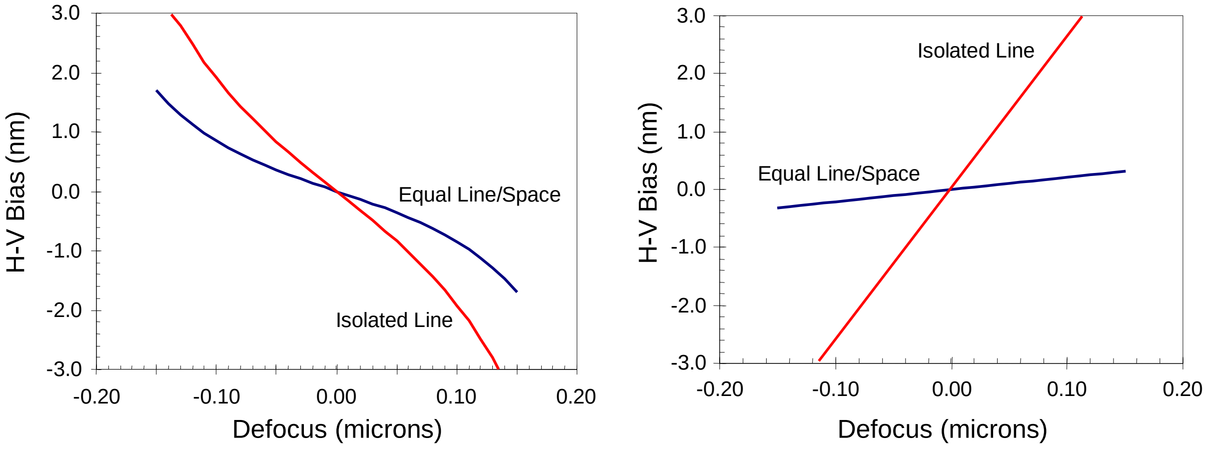

(a) (b)

Figure 2. PROLITH simulations of H-V bias through focus showing approximately linear behavior (λ = 193nm, NA = 0.75, 150nm binary features, 20 milliwaves of astigmatism). a) conventional illumination with σ = 0.6, and for b) quadrupole illumination with σ = 0.65/0.25. For the conventional illumination case, simulations of CD through focus and fits to equation (4) gave the CD curvature parameter a = -184μm^{-2} for the dense features and -403 μm^{-2} for the isolated lines.

Figure 2 shows how strong the influence of the a parameter is. For the conventional illumination case shown here (Figure 2a), the curvature of the CD through focus behavior is about twice as large for the isolated line as the dense lines, resulting in about twice as much H-V bias. For the quadrupole case (Figure 2b), the dose chosen provides an almost isofocal behavior for the dense lines, such that a is almost zero. Thus, the dense features show almost no H-V bias through focus even though the lens has astigmatism. The isolated line, on the other hand, shows significant H-V bias.

Will H-V bias due to astigmatism be a major concern now or in the near future? We can use equation (5) to help answer this question. Let the maximum possible value of the defocus be one-half of the depth of focus (DOF). At this defocus, equation (4) would tell us that at the worst case dose the term $a\delta^2$ will be about 10% of the nominal CD (by definition of the process window with a ±10% CD specification). Thus, we can say that within the process window the worst case H-V bias due to astigmatism will be

$$\left.\frac{H-V\ bias}{CD_{\text{nominal}}}\right|_{\text{max}} \approx \frac{1.6\, Z_{astig}\lambda}{DOF\ NA^2} \qquad (6)$$

Let's plug in some typical numbers for a 65nm process. For a wavelength of 193nm, an *NA* of 0.9, and assuming a depth of focus of 200nm, the fractional H-V bias will be about $2Z_{astig}$. If we are willing to give 1% CD error to H-V bias, our astigmatism must be kept below 5 milliwaves. In general, equation (6) shows that as new, higher resolution scanners are designed and built, the astigmatism in the lens must shrink as fast or faster than the depth of focus of the smallest features to be put into production. So far, lens makers have been successful at achieving this kind of aberration scaling.

3. Source Aberrations

The second major cause of H-V bias is illumination aberrations (that is, source shape asymmetries). Consider conventional illumination where the center of the disk-shaped source is not perfectly aligned with the center of the optical path (called an illumination telecentricity error). For the simple case of dense line/space patterns where only the zero and the two first diffraction orders are used in the imaging, the image will be made up of combinations of one, two and/or three beam interference. Figure 3 shows an example of how an offset in the position of the source (in this case, to the right) changes the relative amounts of two beam and three beam imaging.

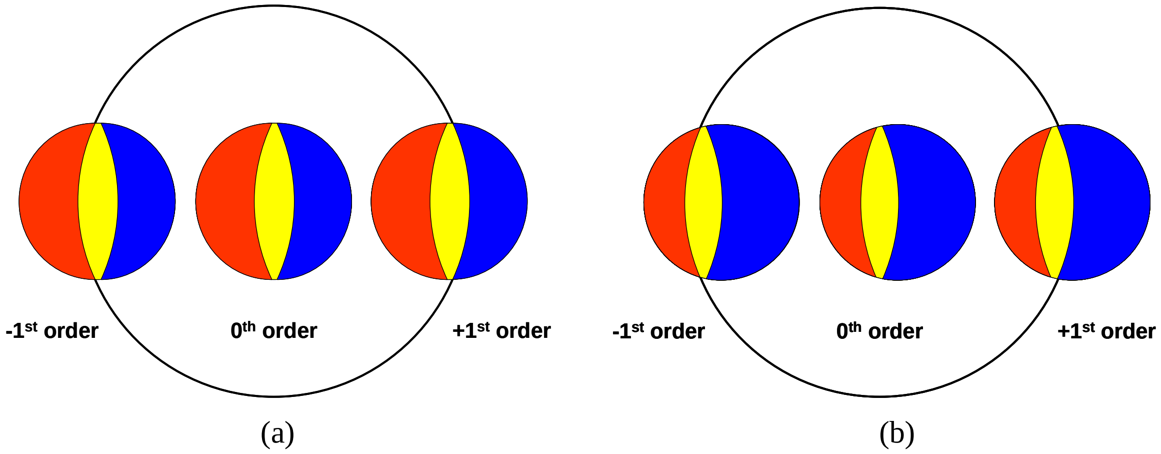

Figure 3. Example of dense line/space imaging where only the zero and first diffraction orders are used. Yellow represents three beam imaging, red and blue show the area of two beam imaging. a) source shape is properly centered, b) source is offset in x (to the right). Note that the diffraction pattern represents vertical (y-oriented) features.

The impact of such a source telecentricity error is dependent on the partial coherence, the pitch, and of course on the amount of telecentricity error. Figure 4 shows that, in general, an x-shift of the center of the illumination source shape affects vertically oriented (y-oriented) lines significantly, but horizontal (x-oriented) lines very little.

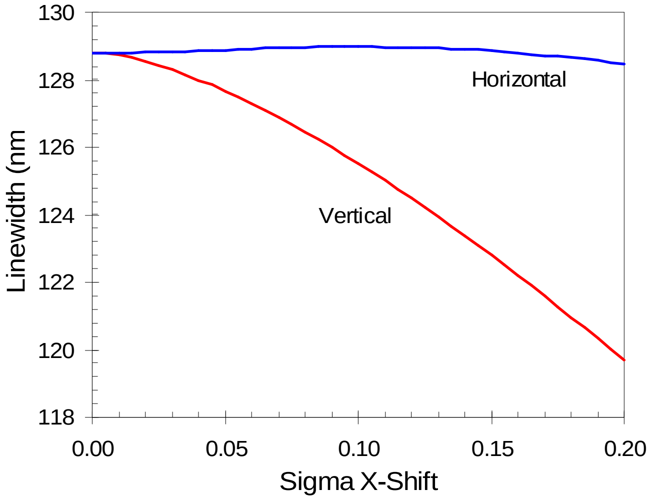

Figure 4. Example of how an x-shift in the center of a conventional source ($\sigma = 0.6$) affects mainly vertical (y-oriented) lines and spaces (CD = 130nm, pitch = 650nm, PROLITH simulations).

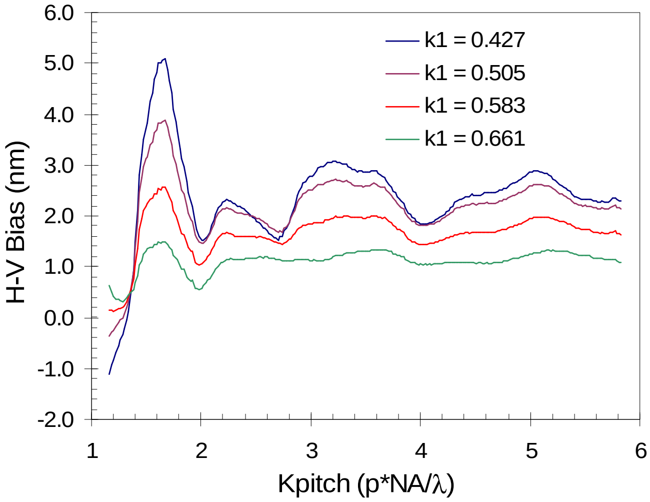

Figure 5. H-V bias as a function of pitch for different feature sizes ($\sigma = 0.4$, x-shift = 0.1).

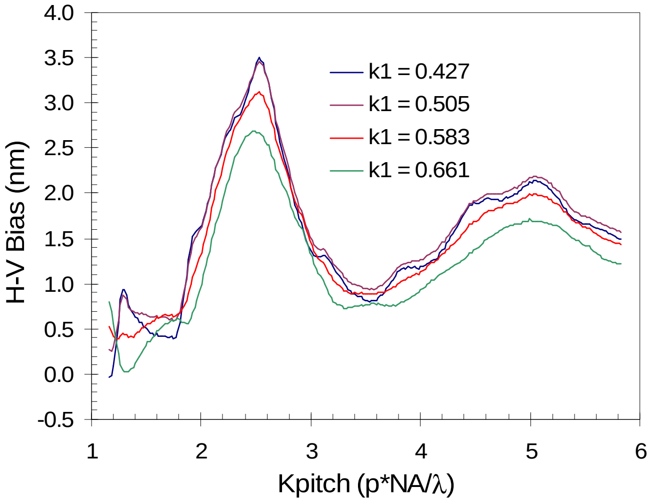

Figure 6. H-V bias as a function of pitch for different feature sizes (σ = 0.6, x-shift = 0.1).

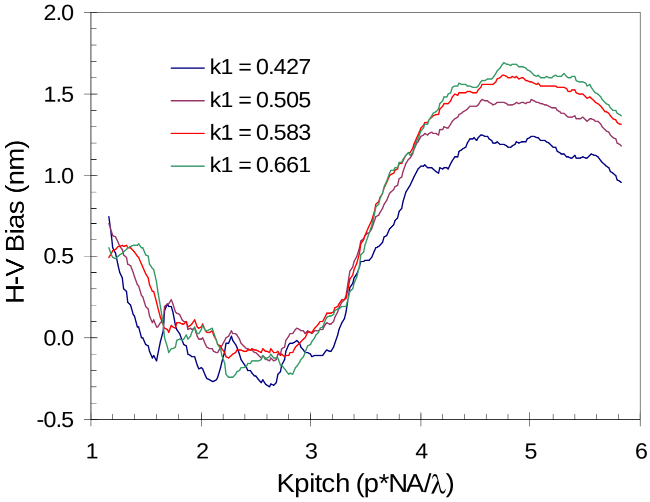

Figure 7. H-V bias as a function of pitch for different feature sizes (σ = 0.8, x-shift = 0.1).

Figures 5-7 explore the pitch dependence on H-V bias for a given amount of telecentricity error. Several important conclusions can be drawn from these simulation results. First, the smaller partial coherence cases show more H-V bias. The worst case H-V bias goes from 5nm for the σ = 0.4 case to 3.5nm for σ = 0.6 and down to 1.7nm for σ = 0.8. Second, there is a weak feature size dependence. Smaller features show slightly more H-V bias. But the feature size dependence is small compared to the pitch dependence. For each sigma value there is a pitch which gives the maximum H-V bias for an illumination telecentricity error. For σ = 0.4 the worst case H-V bias occurs at K_{pitch} (pNA/λ) = 1.65. For σ = 0.6 the maximum H-V bias occurs at K_{pitch} = 2.5. And for σ = 0.8 the maximum H-V bias occurs at about K_{pitch} = 4.8. Other simulations show that this most sensitive pitch is essentially independent of the magnitude of the telecentricity error.

What causes one pitch to have a more sensitive H-V bias response to source telecentricity errors than all the others? The change in CD for the vertical features for an x-shift in the source center is caused by a change in the ratio of two beam to three beam imaging. Figure 3 above showed an example case where the total three-beam imaging area (in yellow) and the total two beam imaging area (red + blue) does not appreciably change as the center of the source is shifted by about 0.1 sigma. Consider a different pitch, as shown below in Figure 8a. At this pitch, all of the first order is inside the lens, so that all of the imaging is three beam (note that the second diffracted order is not shown in the diagram for clarity's sake). However, when the source is shifted in x by 0.1 sigma (Figure 8b), the amount of three beam imaging for the vertical lines is reduced and two beam imaging is introduced. By contrast, the horizontal lines (which spread the diffraction pattern vertically in the pupil) have only an imperceptible change in the amount of three beam imaging for the same x-shift of the source position (Figures 8c and 8d).

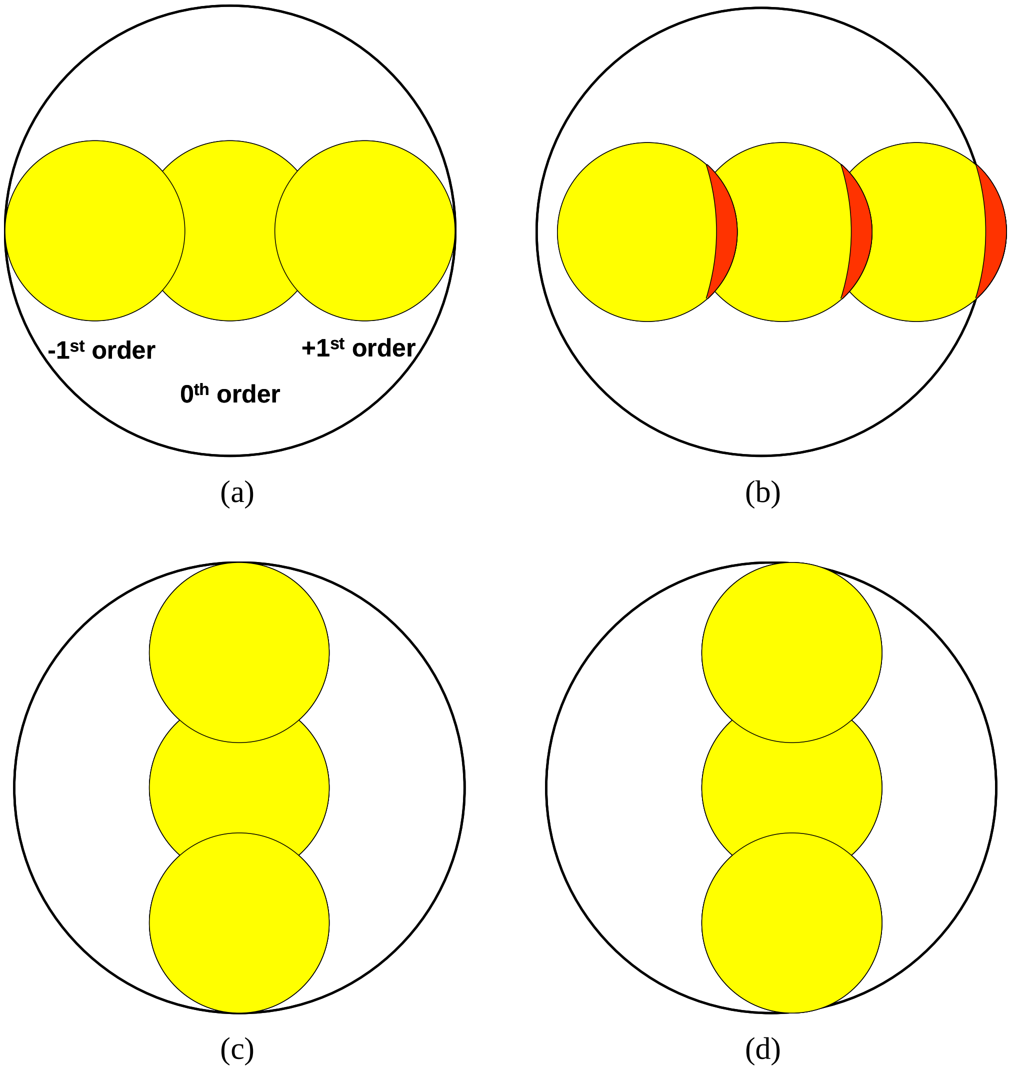

(a) (b)

(c) (d)

Figure 8. Examples of how a telecentricity error affects the ratio of two beam to three beam imaging (σ = 0.4, x-shift = 0.1). a) vertical lines, no telecentricity error, b) vertical lines, with telecentricity error, c) horizontal lines, no telecentricity error, and d) horizontal lines, with telecentricity error.

The pitch that just allows only three beam imaging for a given partial coherence is the pitch that is most sensitive to a shift in the source position. Thus, the worst case pitch from an H-V bias telecentricity error sensitivity perspective is given by

$$\text{worst case } K_{pitch} = \frac{pNA}{\lambda} \approx \frac{1}{1-\sigma} \tag{7}$$

For σ = 0.4, 0.6, and 0.8 this corresponds to worst case K_{pitch} equal to 1.67, 2.5, and 5, respectively, corresponding almost exactly with the simulation results seen in Figures 5-7.

4. Conclusions

There are two major sources of H-V bias in optical lithography: astigmatism coupled with defocus, and illumination source shape errors. Astigmatism causes a shift in best focus as a function of line orientation. If the feature in question is not at its isofocal dose, then a change in focus results in a nearly quadratic change in CD. Thus, astigmatism will cause an H-V bias, the magnitude of which will vary about linearly with defocus. In fact, a measurement of H-V bias as a function of defocus can be used to determine the approximate amount of astigmatism in a lens.

The second major cause of H-V bias is source shape error. As the simulations and analysis above have shown, source errors can cause a change in the ratio of two beam to three beam imaging, affecting vertical and horizontal lines differently. The most sensitive pitch for a given value of partial coherence will be the pitch that puts all of the first order just inside the lens. While the study presented here examined illumination telecentricity error, the results should be similar for other shape errors, such as a deviation from the circularity of the source. If the source were ellipse shaped, with the x-width of the source different from the y-width, similar H-V bias trends should be observed as for a source center shift.

For low levels of objective lens astigmatism and well designed and maintained illumination systems, the amount of H-V bias should be small. However, small is a relative term. For the σ = 0.6 case presented here, 1nm of H-V bias can result from only 0.04 sigma shift in the center of the source. Are source shapes and alignments controlled to this level? That is a question that requires more characterization and measurement of illumination source shapes in real world lithographic systems.

5. References

1. D.S. Goodman and A.E. Rosenbluth, "Condenser Aberrations in Köhler Illumination", *Optical/Laser Microlithography, Proc.*, SPIE Vol. 922 (1988) pp. 108-134.
2. G.J. Stagaman, R.J. Eakin, J.C. Sardella, J.R. Johnson, C.R. Spinner, "Effects of Complex Illumination on Lithography Performance", SPIE Vol. 2726 (1996) pp. 146-157.
3. S.P. Renwick, S.D. Slonaker, I. Lalovic, K. Ahmed, "Influence of Laser Spatial Parameters and Illuminator Pupil-Fill Performance on the Lithographic Performance of a Scanner", *Optical Microlithography XV, Proc.*, SPIE Vol. 4691 (2002) pp. 1400-1411.
4. G. Zhang, C. Wang, C. Tan, J. Ilzhoefer, C. Atkinson, S.P. Renwick, S.D. Slonaker, D. Godfrey, C. Fruga, "Illumination Pupil Fill Measurement and Analysis and its Application in Scanner V-H Bias Characterization for 130nm Node and Beyond", *Optical Microlithography XVI, Proc.*, SPIE Vol. 5040 (2003) pp. 45-56.

5. C. Hwang, I.S. Kim, S.G. Woo, H.K. Cho, W.S. Han, “Impact of Illumination Intensity Profile on Lithography Simulation”, *Optical Microlithography XVII, Proc*., SPIE Vol. 5377 (2004) pp.1427-1434.
6. J. Shin, S. Lee, H. Kim, C. Hwang, S.S. Kim, S.G. Woo, H.K. Cho, J.T. Moon, “Measurement Technique of Non-telecentricity of Pupil-fill and its Application to 60nm NAND Flash Memory Patterns”, *Optical Microlithography XVIII, Proc*., SPIE Vol. 5754 (2005) pp.294-302.